Emergent Materials (2025) 8:2695–2708
https://doi.org/10.1007/s42247-024-00673-6

ORIGINAL ARTICLE

Clean modification of potato starch to improve 3D printing of potential bone bio-scaffolds

Pedro Augusto Invernizzi Sponchiado[1,4] · Maryanne Trafani de Melo[1] · Bruna Sousa Bitencourt[2] · Jaqueline Souza Guedes[2] · Delia Rita Tapia-Blácido[1] · Pedro Esteves Duarte Augusto[3] · Ana Paula Ramos[1] · Bianca Chieregato Maniglia[1,4]

Received: 17 January 2024 / Accepted: 4 March 2024 / Published online: 15 March 2024

Abstract
Although the 3D printing of biomaterials has witnessed remarkable advancements, there is still a need to develop appropriate bio-based inks. Starches are interesting alternatives to produce hydrogels to be used as inks, but native starches rarely present good performance in 3D printing. To bridge this gap, our study innovatively explores new avenues for the utilization of natural biopolymers in biomedical applications. In this sense, we applied the dry heating treatment (DHT) as a "clean" method to modify potato starch for use in the 3D printing of bone bio-scaffolds. Firstly, the effect of the DHT (1, 2, and 4 h at 130 °C) process was evaluated on the structure and physicochemical properties of starch and their hydrogel. Then, 3D-printed bio-scaffolds were obtained from the hydrogels and evaluated in relation to their mechanical performance. DHT promoted starch molecule oxidation and partial depolymerization. The molecular changes resulted in new properties for the obtained hydrogels, such as firmness, cohesion energy, storage modulus (G'), and improved 3D printability—with better accuracy and geometry fidelity. The 3D-printed bio-scaffolds based on DHT starches showed a reduction in the biodegradability rate in relation to the native starch, reducing the swelling power, and improving the mechanical performance—in special DHT 130 °C for 1 h. In conclusion, the DHT process is a "clean" and effective method to modify potato starch not only to enhance the performance of the hydrogels but also to improve the properties of the printed biomaterials.

Keywords Modified starch · Hydrogels · 3D printing · Biomaterials

1 Introduction

3D printing is an advanced technology that enables the automated and reproducible production of functional, scalable, and customized artificial structures for personalized materials [1]. This cutting-edge technology uses layer-by-layer deposition of biocompatible materials to create stable 3D constructs for biomedical applications.

For instance, bone bio-scaffolds can be produced by extrusion-based bioprinting, using biocompatible hydrogels [2, 3]. By utilizing this method, different tissues can be printed with anatomically accurate macroporous structures [4]. However, there are only a limited number of biomaterials suitable for ink formulations because they must be printable, biocompatible, and have favorable structural and mechanical properties [5].

Starch is a natural, biocompatible, and biodegradable polymer that is cheap and widely available and is an interesting gelling ingredient for 3D printing applications, from

✉ Bianca Chieregato Maniglia
biancamaniglia@iqsc.usp.br

1 Departamento de Química, Faculdade de Filosofia, Ciências e Letras de Ribeirão Preto–FFCLRP, Universidade de São Paulo–USP, Avenida Bandeirantes, Ribeirão Preto, SP 14040-900, Brazil

2 Departament of Agri-food Industry, Food and Nutrition (LAN), Luiz de Queiroz College of Agriculture (ESALQ), University of São Paulo (USP), Piracicaba, SP 13418900, Brazil

3 Université Paris-Saclay, CentraleSupélec, Laboratoire de Génie des Procédés et Matériaux, Centre Européen de Biotechnologie et de Bioéconomie (CEBB), 3 rue des Rouges Terres 51110, Pomacle, France

4 São Carlos Institute of Chemistry, University of São Paulo–USP, Av. Trabalhador São-Carlense, Sao Carlos, SP 13566-590, Brazil

food to biomedical [6–8]. However, despite its promising results, native starches have presented limitations for 3D printing, such as processing difficulties, high swelling, high hydrophilic character, low mechanical resistance, and instability for long-term applications [9]. For instance, potato starch has been proposed to be used in the 3D printing of biomaterials [10], but with many limitations, such as poor heat stability and rheology unfavorable for 3D printing applications [11]. In fact, Chuanxing et al. [12] recently needed to combine proteins, a noble biomacromolecule, with potato starch to obtain adequate printability.

In this context, starch modification methods can be explored to overcome the deficiencies of native starches and offer a promising avenue for improving the 3D printing performance of inks used in the fabrication of biomaterials, thus advancing the field of tissue engineering.

Among different starch modification processes, dry heating treatment (DHT) involves a straightforward, physical, simple, and safe technique to modify starch's structural and physical-chemical properties [13], which can be used for food, biomedical, and pharmaceutical applications. In fact, this technique is considered a "green and clean technology" that does not generate effluents to be treated, and the obtained products do not present traces of chemical components [9]. Although DHT has been proposed to modify other starch sources [14–18], it has not been evaluated so far to modify potato starch, mainly in the context of 3D printing of biomaterials.

In fact, each starch source reacts differently to DHT, and potato starch presents some specificity that makes it unique—highlighting the need to evaluate the DHT processing of this source. Potato starch is characterized by large particle size, long amylose and amylopectin chain lengths, and the presence of phosphate ester groups, which affects its dough and gelatin properties compared to other sources [14, 19].

Despite the increased number of studies on inks for 3D printing, there remains a significant gap in developing bio-inks to obtain biomaterials with enhanced properties. In order to overcome this gap, our study innovatively explores new avenues for the utilization of natural biopolymers in biomedical applications. In this work, we evaluated the DHT modification process of potato starch, processed at different conditions, with focus on 3D printing of bone bio-scaffolds as a biomaterial application. Our analysis focused on the impact of DHT on the structural and physicochemical properties of potato starch, including 3D printability, aiming to establish a connection between these properties and the printing performance. At final, we evaluated the effect of DHT in the performance of the printed potential bio-scaffolds.

2 Material and methods

2.1 Material

Native potato starch (moisture content: 11.1 g/100 g, apparent amylose: 22.6 g/100 g starch, d.b.) was purchased from Cargill–Agrícola (Brazil). All the chemical reagents were of analytical grade. All the aqueous solutions were prepared with ultrapure dust-free water from a Milli-Q® system (resistivity = 18.2 MΩ cm). The reagents used in this work were sodium chloride (NaCl, Synth-Diadema, Brazil, 99.5%), sodium hydroxide granular (NaOH, Synth-Diadema, Brazil, P.A.), dimethyl sulfoxide (DMSO, Synth-Diadema, Brazil, 90%), Sepharose CL-2B gel (Sigma, Sweden), absolute ethanol (Êxodo Cientifica, Brazil, P.A.), and hydroxylamine hydrochloride (Sigma-Aldrich, USA, 99%).

2.2 Starch modification

The dry heating treatment (DHT) followed the method described by Maniglia et al. [16]. In summary, the experimental procedure involved the following steps: first, a layer of potato starch powder was evenly spread (~1.0–1.5 mm) onto a sheet of aluminum foil. Then, another sheet of aluminum foil was placed over it to cover the thickness. The lateral parts of the structure were sealed with tape to create a closed envelope that prevents any loss of material. Next, the sealed starch sample was placed in a hot-air convective oven (ModFic03, Famo, São Paulo, Brazil) for the process of dry heating treatment (DHT). The DHT involved exposing the starch to hot air at a temperature of 130 °C for different periods: 1, 2, and 4 h, referred to as DHT_1h, DHT_2h, and DHT_4h, respectively. After the DHT process, the modified starch was allowed to cool and then stored in glass containers for subsequent analysis. The moisture content of native and modified potato starches was analyzed in a moisture analyzer Mb27 OHAUS (Barueri, Brazil). Under constant stirring, a potentiometer (Tecnal, model TEC-5 mode, Piracicaba–Brazil) was employed to determine the pH of the starch suspension (10.7 g starch/100 g suspension).

2.3 Modified starch characterization

2.3.1 Molecular properties: carbonyl and carboxyl groups and molecular size distribution

The molecular size distribution profile was determined using a gel permeation chromatography (GPC) system, according to Song and Jane [20], with some modifications described by Maniglia et al. [17]. The glass column used in the experiment was GE Healthcare–28988950 XK 27/70, which was

packed with Sepharose CL-2B gel sourced from Sigma (Sweden). To begin, a solution was prepared by combining 0.1 g of starch with 10 mL of dimethylsulfoxide (DMSO; 90% from LabSynth, Brazil). This starch-DMSO mixture was then subjected to heat by immersing it in a boiling water bath for 1 h. Afterward, the solution was allowed to cool to 25 °C and stirred continuously for 24 h. Next, 3 mL of the prepared starch solution was mixed with 10 mL of absolute ethanol and centrifuged for 30 min at 3000 g. The resulting precipitated starch was dissolved in 9 mL of water and then heated in a boiling water bath for 30 min. Subsequently, a 4 mL portion of this starch solution was added to the chromatographic column. The eluent solution used in the column consisted of 25 mmol·L^{-1} of NaCl and 1 mmol·L^{-1} of NaOH. The starch solution was introduced into the column at a rate of 1 mL·min^{-1}. During the process, aliquots of 4 mL were collected using a fraction collector (Gilson, model FC203B, Middleton, England). These collected samples were then subjected to analysis using the blue value method [21]. The analysis involved measuring the absorbance of the samples at a wavelength of 620 nm using a spectrophotometer (Femto, model 600S, São Paulo-Brazil). Glucose was used as a marker to indicate the completion of the analysis.

The carbonyl and carboxyl contents were determined according to the methods described by Smith [22] and Chattopadhyay et al. [23], respectively. The methods were well described in the work of Lima et al. [24]. The result is expressed in terms of the amount of carboxyl groups per 100 glucose units (COOH/100 GU).

2.3.2 Starch pasting and hydrogel properties (firmness and rheology)

Starch parting properties were determined using a Rapid Visco Analyzer (RVA) (Newport Scientific Pvt. Ltd., Australia, with thermocline for Windows software, version 3.0). Standard starch characterization conditions were used with a suspension of 10.7 g starch/100 g (corrected to 14% moisture). The steps of the procedure were as follows: hold at 50 °C for 1 min, then heat to 95 °C (6 °C-min^{-1}) and hold at 95 °C for 5 min, then cool at 50 °C (6 °C-min^{-1}), and finally hold at 50 °C for 2 min. To avoid misunderstandings, important parameters were calculated, such as relative breakdown (RBD) and relative setback (RSB). The relative breakdown (RBD) was calculated by the ratio between the breakdown (BD) and the apparent peak viscosity (PAV) to understand the ease of starch granule breakup. Relative setback (RSB) was calculated by the ratio between the values of setback (SB) and TAV (through apparent viscosity) to understand the tendency to retrograde.

Hydrogels based on the starches (the same formulation to be used as inks in the 3D printing of the bio-scaffolds) were produced to characterize the rheological properties and firmness. The starch hydrogels were prepared by adding potato starch (10 g/100 g d.b.) to water and heating the suspension at 85 °C in a bath (Solidsteel, Brazil) under constant agitation with a mechanical agitator (Fisatom Scientific, Brazil) for 30 min. After this, the starch paste was taken in plastic molds (20 × 20 mm, diameter × height) and in syringes (5 mL), which were maintained in desiccators with water at 5 °C for 24 h. After this time, the native and modified starch hydrogels (DHT_1h, DHT_2h, DHT_4h) were obtained. The hydrogels in the molds were used for rheology and gel firmness characterization. The hydrogels in the syringes were used for printing the bio-scaffolds.

The hydrogel rheology was analyzed in a hybrid rheometer (Discovery HR-3, DHR, TA Instruments, USA) using a 20 mm parallel plate with 2000 µm of gap at 25 °C. Before testing, excess material off the plate was scraped off and allowed to rest for 5 min to unstring the structure and reach the desired temperature. Both steady-state flow and viscoelastic properties were evaluated.

Flow ramps were conducted at shear rates of 0.1 to 100 1/s, which were fitted to the Power-Law model as follows:

$$\eta = K\gamma^{n-1} \quad (1)$$

where η represents the apparent viscosity of the ink (Pa·s), K is the consistency index of the hydrogel (Pa.s^n), γ is the shear rate (s^{-1}), and n is the flow behavior index (dimensionless).

Dynamic vibration frequency analysis was performed at a constant deformation (0.03% strain, within the linear viscoelastic range) with a frequency from 0.01 to 100 Hz. The mechanical spectra were obtained by recording the storage modulus (G') and the loss modulus (G'') as a function of frequency. Furthermore, the loss factor, represented by tan δ = (G''/G'), was determined by analyzing the plateau region of the storage modulus (G') and loss modulus (G'') as a function of frequency.

The strength of the hydrogels was determined by a puncture test using a texture analyzer TA TX Plus (Stable Micro Systems Ltd., Surrey, UK) with a load cell of 50 kgf (490.3 N). Specimens were penetrated with a cylindrical probe (P/0.5 R, 0.5 in. diameter) at 1 mm.s^{-1} to a distance of 10 mm. The instrument measures the force as a function of penetration depth. Strength is associated with the maximum force at a given distance, and cohesive energy was determined by the area under the graphical force × penetration depth (fixed at 10 mm).

2.4 Bio-scaffold production and ink performance

The native and modified starch hydrogels, described in section 2.3.2, were used as the inks for bone bio-scaffold production. The hydrogels conditioned in the syringes (5 °C/24 h) were printed using a 3D printer of the bioV4-BioEdPrinter

v4-4 Modular extrusion type of BioEdTech (São Paulo-SP, Brazil). The bone bio-scaffolds were printed, at room temperature, according to the following pre-optimized parameters: robotic arm speed = 10 mm/s; extrusion flow (w) = 100%; needle diameter (d) = 1.2 mm; 3D geometry = parallelepiped (20 × 20 × 2 mm) with filling percentage = 15% and rectangular geometry filling. The 3D-printed project was a parallelepiped with 4 cm^2 of surface area and 88 orifices in its structure, a geometry frequently used for food and biomedical applications.

The ink's performance was evaluated by reproducibility of the 3D-printed bio-scaffolds and its fidelity with the original project. The samples were weighed on an analytical balance (AUW220D, Marte Científica, Minas Gerais, Brazil), the sizes were measured in five different positions using a digital caliper (CD-6 CSX-B model, Mitutoyo, Roissy-en-France, France), and the surface area was calculated by image processing using the ImageJ software.

We also calculated the geometry fidelity (GF) based on the comparison between the surface area of the 3D-printed parallelepiped and the area of the project (Eq. 2) and the number of orifices (N) of the 3D-printed parallelepiped and the number of orifices of the project (Eq. 3).

$$\mathrm{GF}_{\mathrm{area}} = \left(\frac{\mathbf{Area}_{\mathbf{printed\ parallelepiped}}}{\mathbf{Area}_{\mathbf{parallelepiped\ 3D\ project}}} \right) \times 100 \tag{2}$$

$$\mathrm{GF}_{\mathrm{orifices}} = \left(\frac{\mathbf{N}_{\mathbf{printed\ parallelepiped}}}{\mathbf{N}_{\mathbf{parallelepiped\ 3D\ project}}} \right) \times 100 \tag{3}$$

Once printed, the bio-scaffolds were immediately frozen (−18 °C for 24 h) and then freeze-dried (vertical lyophilizer model SL-404, Solab, Brazil). The lyophilized bio-scaffolds were preconditioned (58% RH, 25 °C) for subsequent characterizations.

2.5 Bio-scaffold characterization

2.5.1 Mechanical properties

The thickness of the preconditioned bio-scaffolds (58% RH, 25 °C) was evaluated through the average thickness resulting from five measurements at random positions using a digital micrometer (model CD-6 CSX-B, Mitutoyo, Roissy-en-France, France) with a flat tip (resolution of 1 µm). The bio-scaffolds were also assessed in their mechanical properties using a puncture test, similar to reported by Sobral et al. [25] and La Fuente [26]. The force applied for punching (F) (N) and deformation at the scaffold breaking point (D) (mm) was determined in a Texturometer (TA Instrument–TA. TX Plus, with a load cell of 30 kgf/294 N), using the "Texture Expert" software. For this purpose, the bio-scaffolds were fixed in circular permeation cells (d = 0.05 m) and perforated with a probe of 3 mm diameter.

2.5.2 Biodegradability and swelling

Bio-scaffolds were placed in sterile 6-well plates for cell culture and immersed in 5 mL of sterile cell culture medium (α-MEM, Gibco) at 37 ± 2 °C under 5% CO_2 atmosphere for 7 and 14 days. The entire procedure was performed in a laminar flow chamber to avoid contamination. Afterward, the bio-scaffolds were collected and completely dried in an oven. Biodegradability was calculated based on the percentage of mass dissolved in the medium during the respective time interval. To determine the rate constant for scaffold biodegradation over time, we employed a curve-fitting model. This process was conducted in batch mode, and we applied the dynamic mass balance for scaffold degradation, which follows the first-order reaction model as presented in Eq. 4.

$$-r_A = \frac{dB}{dt} \tag{4}$$

In this context, biodegradability B (%) represents the mass of biodegraded bio-scaffolds at time t (h), while $-r_A$ (%.h^{-1}) signifies the rate of scaffold biodegradation in the cell culture medium. We tailored the biodegradation profile by adhering to a first-order reaction model and estimated the duration required to achieve complete biodegradation (100%).

For swelling evaluation, the bio-scaffolds were weighed and immersed in α-MEM medium in sterile 6-well plates for cell culture, and photos were taken at periods of 0, 2, 4, 8, 24, 48, and 72 h of immersion. The images were processed by ImageJ software to calculate the variation in the area of the scaffold (A_{initial}: initial area before immersion in the middle and A_{final}: final area after immersion), with swelling power (SP) being calculated as shown in Eq. 5.

$$\mathrm{SP}\ (\%) = \frac{\left(A_{\mathrm{final}} - A_{\mathrm{initial}}\right)}{A_{\mathrm{initial}}} * 100 \tag{5}$$

2.6 Experimental design and statistical analysis

All experiments were repeated three times, and the average data were used to plot the curves which are shown in the tables. All processes and analyses were performed in triplicate in a completely randomized design, and results were expressed as mean ± standard deviation. To determine statistical differences, results were analyzed by analysis of variance (ANOVA) and Tukey test at 5% significance using Minitab® software (version 19.2, USA).

3 Results and discussion

3.1 Modified starch characterization

3.1.1 Molecular properties

The degree of oxidation was evaluated by the molecular carbonyl and carboxyl contents, as well as the suspension pH (Table 1). DHT promoted oxidation in potato starch, with an increase in the carbonyl content, but without reaching carboxyl group formation and with no significant difference in the pH (Table 1). Therefore, the oxidation promoted by DHT was mild, similar to the observed for cassava starch by Maniglia et al. [16] and Lima et al. [24], but different to the observed for maize starch [27].

Figure 1 shows the molecular size distribution of native and modified potato starch. GPC analysis was performed to determine the molecular size distribution, which is a size exclusion technique. In this technique, starch molecules are placed in a column filled with a gel of a certain porosity: larger molecules elute first, while smaller molecules are retained in the pores of the gel and elute later [27]. The first peak of the graph (first fractions) refers to the larger molecules that can be associated with amylopectin molecules, while the second peak refers to the smaller molecules that can be associated with the amyloses [26].

As the DHT time increased, the modified starches showed a reduction of the first peak (Fig. 1), indicating that the fraction of larger-sized molecules was partially cleavage. Indeed, the second peak was increased (the fraction of small molecules), and both the first and second peaks shifted to the right (longer elution times). This suggests that DHT promotes the formation of smaller molecules (retained longer in the chromatographic column) due to partial depolymerization by glycosidic bond cleavage. These results are consistent with the work in which DHT was used in wheat and cassava starch [16, 17, 24].

Molecular characterization demonstrates that DHT affects the different levels of the starch molecules, which is more drastic as the DHT time increases. Consequently, further evaluation is needed to verify if the changes at the molecular level can affect the starch functional properties—as described in the next sections.

Table 1 pH, carbonyl, and carboxyl content of the native and modified potato starches (DHT_1h, DHT_2h, and DHT_4h) (average ± standard deviation)

Samples	pH	Carbonyl content (CO/100 GU)	Carboxyl content (COOH/100 GU)
Native	5.32 ± 0.23^{a}	0.014 ± 0.007^{d}	0.000 ± 0.000^{a}
DHT_1h	5.10 ± 0.25^{a}	0.033 ± 0.001^{c}	0.000 ± 0.000^{a}
DHT_2h	4.95 ± 0.18^{a}	0.053 ± 0.002^{b}	0.000 ± 0.000^{a}
DHT_4h	4.98 ± 0.25^{a}	0.075 ± 0.001^{a}	0.000 ± 0.000^{a}

a, b, c, d: different letters indicate significant differences between the native and the modified starches, as revealed by Tukey's test, $p < 0.05$

3.1.2 Starch pasting and hydrogel properties (firmness and rheology)

Figure 2 and Table 2 show, respectively, the RVA curves and their associated parameters for the native and modified potato starches.

The paste temperature (PT) corresponds to the temperature at which starch granules begin to swell due to water absorption [28]. The increase in DHT time resulted in an increase in the PT value, which could be related to the presence of a high proportion of small molecules that require more energy to gelatinize than large molecules, similar to what was observed by Lima et al. [24].

The PAV (peak apparent viscosity) represents the maximum apparent viscosity of the pasting reached in the heating step when the starch grains absorb water and swell. It indicates the point between the maximum swelling and the rupture of the granules [28]. Figure 2 and Table 2 demonstrate that as DHT time increased, the PAV decreased drastically.

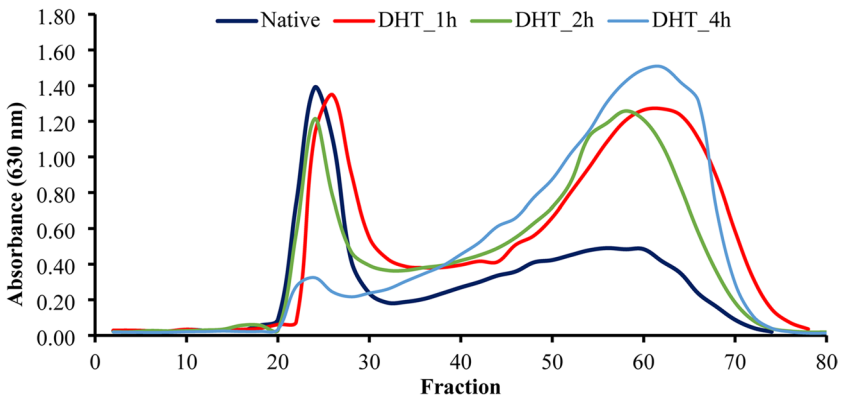

Fig. 1 Molecular size distribution of the native and modified potato starches (DHT_1h, DHT_2h, and DHT_4h)

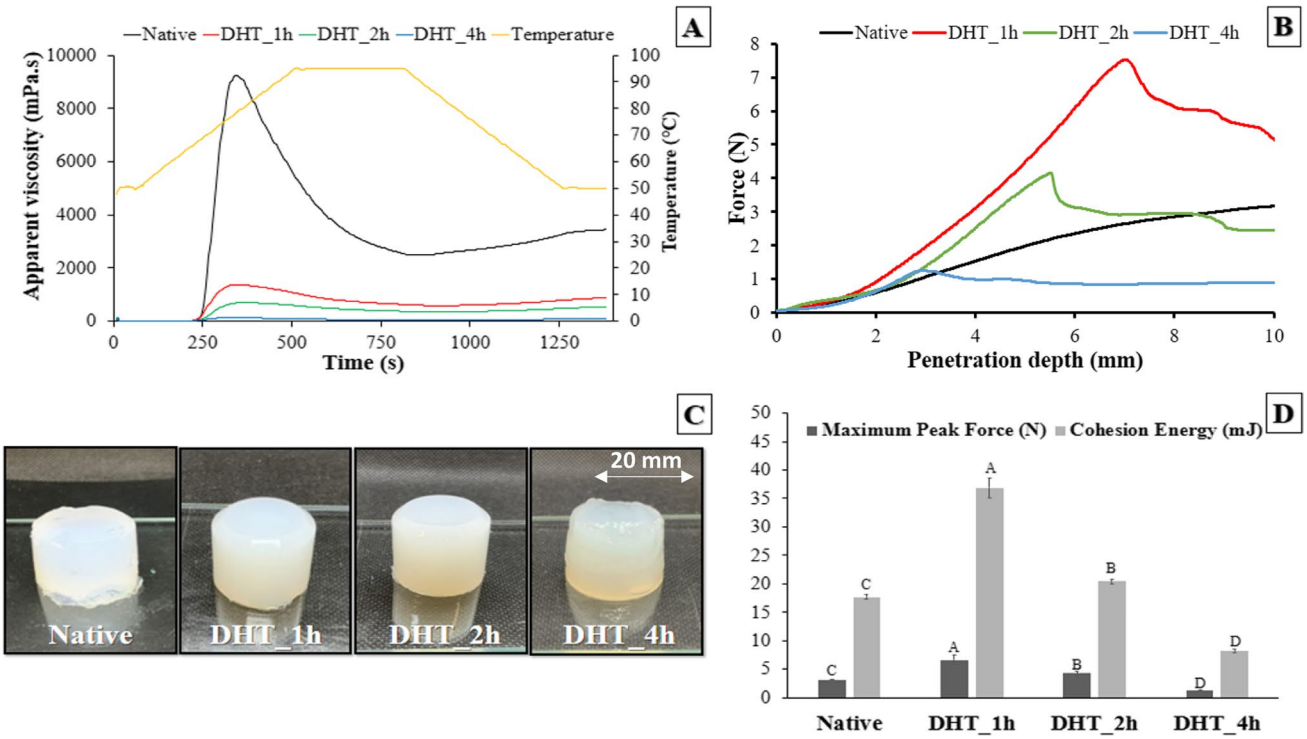

Fig. 2 **A** RVA curves, **B** force vs penetration depth, **C** images of the molded gels obtained, and **D** maximum peak force and cohesion energy of the native and modified starches (DHT_1h, DHT_2h, and DHT_4h). (A–D) Different letters indicate significant differences between the native and the modified starches, as revealed by Tukey's test, $p < 0.05$

Table 2 Parameters obtained from the RVA of the native and modified potato starches (DHT_1h, DHT_2h, and DHT_4h) (average ± standard deviation)

Samples	PAV (mPa.s)	RBD (%)	RSB (%)	PT (°C)
Native	9245.7 ± 76.8^{A}	38.3 ± 0.76^{C}	73.1 ± 0.26^{A}	67.50 ± 0.04^{C}
DHT_1h	1374.3 ± 2.4^{B}	48.6 ± 0.10^{B}	57.0 ± 0.48^{C}	67.55 ± 0.01^{C}
DHT_2h	702.0 ± 2.9^{C}	52.6 ± 1.30^{A}	50.0 ± 0.58^{D}	68.85 ± 0.33^{B}
DHT_4h	133.7 ± 1.2^{D}	50.3 ± 1.42^{A}	58.9 ± 0.30^{B}	69.55 ± 0.18^{A}

A, B, C, D: different letters indicate significant differences between native and the modified starches (DHT_1h, DHT_2h, and DHT_4h), as revealed by Tukey's test, $p < 0.05$

PAV, peak apparent viscosity; *RBD*, relative breakdown; *RSB*, relative setback; *PT*, pasting temperature

It can be associated with the weakening of the starch granule's structure and the molecular depolymerization with the increase of the DHT time—similar to cassava and wheat starches processed by DHT [16, 17].

The relative parameters RBD (relative breakdown) and RSB (relative setback) were calculated according to the methodology proposed by Castanha et al. [29]. RBD is a parameter related to how ease the granules break up. In addition, RSB is a parameter that indicates the tendency to retrogradation, which consists of the re-association or reordering of starch molecules [30]. As the DHT time increased, there were higher values of RDB, indicating that the modified starch granules were easier to break, and the molecules had a lower tendency to retrograde than the native one—a consequence of the new molecular distribution and chemical interaction.

Figure 2 also shows a graphic of the force versus penetration depth for the obtained hydrogels, as well as the associated maximum force and cohesion energy.

Figure 2D shows that the DHT_1h sample presented higher gel firmness and higher cohesion energy in relation to the other samples. In contrast, the DHT_4h sample presented the lowest value of these parameters. The cohesion energy refers to the energy required to break the gel, so the higher its value, the more difficult it is to break the structure of the gel. These results are in accordance with the analysis of the rheology of the hydrogels once the DHT_1h was the gel that presented the lowest tan δ and DHT_4h, the highest (presented as follows).

The higher hydrogel cohesion energy can be related to better re-association of the starch molecules, with the newly added functional groups and adequate molecular size distribution [24]. In this way, the results indicate that depending on the DHT time, this treatment was able to promote the formation of starch molecules with better (1

h) or worse (2 and 4 h) capacity of re-association than the native potato starch (visible in Fig. 2C). This maximum resistance highlights how the changes promoted by DHT are not linear and a case-by-case study is necessary to achieve the best results for each source and application.

The DHT_2h and DHT_4h exhibited the highest content of carbonyl groups, which can form hydrogen bonds with carbonyl or hydroxyl groups of starch chain segments, resulting in better structural integrity [31]. This may contribute to better re-association of the starch molecules (amylose and amylopectin), but the size distribution of the molecules will affect the overall packing and proximity to interaction. Although a reduction in molecular size can favor the conformation of strong gels as a quilting effect, if the motes present a too-small size, it can vitiate their re-association, as observed for hydrogel grounded on DHT_2h and DHT_4h. On the other side, the profile of molecular size distribution and the carbonyl content of DHT_1h was favorable to promote better structural integrity than the native starch and the other modified starches. A balance, thus, between depolymerization and functional groups will dictate the properties of the obtained hydrogels. Finally, we observed that DHT promoted the formation of potato starches with different properties (paste and hydrogel firmness, in this case) expanding its potential for industrial application.

The syringe-based extrusion printer typically uses high-viscosity gels that are extruded through a die or print head and must have a mechanical property/viscosity that allows for vertical assembly, i.e., self-supporting capability which refers to layer support inferior to the top layer, which is related to shape retention [32]. In this sense, some parameters must be considered for the extrusion technique: ability of the ink to be extruded through the printing matrix; ability of the printed stacked layers to have sufficient mechanical integrity to support them without defects such as sagging and warping; the stability and definition of the printed lines after deposition guarantee good resolution of the printed sample [33]. In this way, rheological properties of the inks can predict the behavior of these formulations in relation to processability and quality of the 3D printing [34].

The analysis of the rheological properties of native and modified starches is shown in Fig. 3. Figure 3A demonstrates the pseudoplastic (shear-thinning) behavior of starch hydrogels, whose parameters of the Power-Law model (R^2 were always close to 0.99) are shown in Table 3—n (flow behavior index) and K (consistency index). All n values were much lower than 1, confirming the shear-thinning behavior, which can be desirable for 3D printing—the material with shear-thinning is fluently extruded at a high shear rate during 3D printing and potentially maintains its structure after deposit [35]. In addition, it is noted that the initial apparent

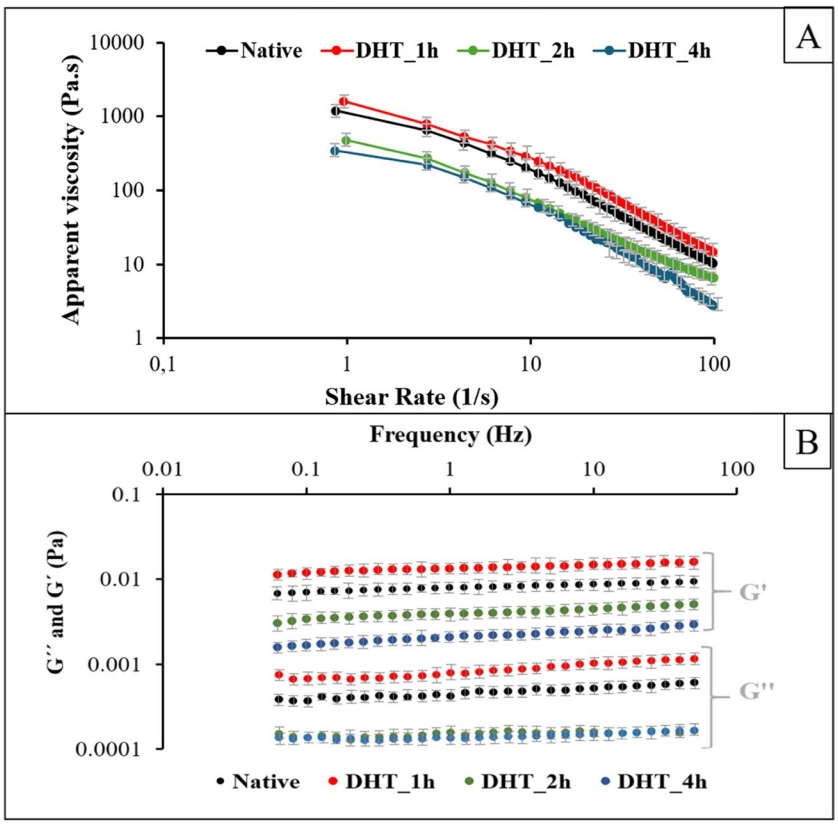

Fig. 3 Rheological properties of native and DHT-modified potato starch: **A** Apparent viscosity variation with the shear rate; **B** storage modulus (G') and loss modulus (G'') as a function of frequency

Table 3 Power-Law parameters and tan δ (G''/G') determined by the medium of G'' and G' in the plateau) of the hydrogel potato starches of the native and modified potato starches (DHT_1h, DHT_2h, and DHT_4h)

Hydrogels	$\eta = K\gamma^{n-1}$			tan δ (G''/G', in the plateau)
	K (Pa·s^n)	n	R^2	
Native	786.16 ± 8.90^b	0.20 ± 0.01^b	0.99	0.0632 ± 0.0007^c
DHT_1h	1597.03 ± 5.67^a	0.33 ± 0.00^a	0.98	0.0382 ± 0.0005^d
DHT_2h	665.49 ± 4.55^c	0.23 ± 0.01^b	0.99	0.0666 ± 0.0004^b
DHT_4h	343.80 ± 9.08^d	0.20 ± 0.00^b	0.98	0.0701 ± 0.0013^a

a, b, c, d: different letters indicate significant differences between native and the modified starches (DHT_1h, DHT_2h, and DHT_4h), as revealed by Tukey's test, $p < 0.05$

viscosity and K values were higher for the DHT_1h samples, and lower for the samples of DHT_4h, in relation to the control, a behavior like those obtained through the penetration assays of the gels (Fig. 2D). Liu et al. [31] indicated that a smaller K value contributes to the smooth extrusion of the starch gel during 3D printing and improves printing precision. Liu et al. [36] observed that Power-Law fluids with K value between 1000 Pa·s^n and 1800 Pa·s^n and the n value between 0.15 and 0.3 showed better printing characteristics, which matches with the profile observed for the DHT_1h. Also, all the inks evaluated in this work showed viscosity (at a shear rate equal to 1 s^{-1}) inside of the viscosity range (30 mPa/s to over 6×10^7 mPa/s) stipulated by Murphy and Atala [37] for potentially suitable use with an extrusion-based 3D printer.

Ahn et al. [38] underlined the importance of the behavior of gel rheology after printing, as it should result in a material that has sufficient self-support to ensure good printability. This behavior can be associated with the elastic or storage modulus of the hydrogels. The elastic or storage modulus (G') represents the material's capacity to store energy during oscillation (solid behavior), while the viscous or loss modulus (G'') determines its ability to dissipate energy because of viscous deformation (fluid behavior). Figure 3B shows that G' is always higher than G'', which denotes that solid/elasticity dominates the gel-like structure. Hydrogels with this behavior have good potential to be used as inks for 3D printing since they can better recover their shape when deposited on the surface [39] (printability was evaluated in the next section).

Table 3 also shows the tan δ parameter (G''/G') of the starch hydrogels. A high value of tan δ (G''/G') indicates that the material has a more fluid appearance, and a low value of tan δ means a more solid material, with low fluidity [35]. In general, all the values of tan δ of the starch hydrogels were less than 1, suggesting the dominant elastic behavior of the materials. However, it is noted that the sample with the lowest tan δ value was the DHT_1h followed by native starch, DHT_2h, and DHT_4h. Therefore, DHT_1h shows a more solid-like behavior while DHT_4h has a more fluid-like behavior. These results suggest that the structural modification of starch granules promoted by DHT altered the viscoelastic properties of the potato starch samples in different ways depending on the DHT time, and how this can affect the printability of these hydrogels will be evaluated in the next section.

To define the self-supporting of printed objects, some authors have suggested using the loss tangent or tan δ as a valuable parameter to describe the shape stability. If the ratio tan $\delta = G'/G''$ is too high, the ink behaves like a liquid and collapses when printed, but the closer tan δ is to zero, and it may present non-homogeneity and require high pressure for processing [40].

In this sense, the tan δ of the starch inks produced in this work showed values close to the lower limit of the tan δ range ($0.052 < \tan \delta < 0.268$) found in the literature for inks with good self-supporting capacity such as sodium alginate, soy protein isolate, gelatin in various concentrations [41], tyramine hyaluronan derivative hydrogels and hydroxypropyl methylcellulose [42], hyaluronic acid [43], alginic acid sodium salt, carboxymethyl (CM) cellulose sodium salt, gelatin type A, and κ-carrageenan [44]. It confirms the potential of starch gels, mainly of the modified starches, to be used as inks in 3D printing, once they show good processability and performance in the final products, but also because they present lower cost and availability when compared to the other sources mentioned.

3.2 Evaluation of the ink's performance

The ink performance is an interesting point to be investigated once that it is a crucial factor to create printed samples with good resolution. In the field of biomedical applications, where precision and accuracy are paramount, obtaining high-resolution prints is essential. A well-designed ink not only contributes to the clarity and fidelity of printed details but also improves the functionality and reliability of the final product, especially when thinking about a personalized biomaterial. The manufacturing of patient-specific constructs or implants accurately imitates the complex and irregular geometric shapes of native tissues, based on computer drawings or medical images. Furthermore, it allows the creation of structures with complex and customizable internal pore networks. These networks can be adapted, adjusting parameters

such as pore size and interconnectivity, to improve nutrient diffusion and support the vitality of embedded cells.

In this sense, Fig. 4 shows pictures of printed geometries based on different native and modified hydrogels, in order to evaluate their potential to be used as inks for 3D printing. Table 4 shows the reproducibility (weight, area, and the number of orifices of the printed samples) and geometry fidelity (GF) in relation to the area (GF_{area}) and the number of orifices ($GF_{orifices}$) of the native and modified potato starch hydrogels. In general, it is relevant to mention that the 3D printing duration of the bio-scaffold was consistently under 3 min (2 min and 55 s) per sample, and there were no apparent indications of natural drying during the 3D printing process.

We can observe in Fig. 4 that the hydrogels based on starches DHT_1h and DHT_2h presented printed geometries with greater definition, with emphasis on the deposition of lines in a continuous manner, with greater definition of the geometry of the orifices. Samples printed with native starch had a flawed printed geometry, while samples printed with DHT_4h, despite having all their geometry printed, formed holes without defining squares, as the rheology of this hydrogel resulted in round holes different from that defined in the project. It is noted that the rheology of the DHT_1h and DHT_2h hydrogels was favorable for use in 3D printing; however, DHT_4h, despite the printed lines being more continuous and smoother, do not support themselves, resulting in holes without project definition. Thus, it can be said that the time of DHT in potato starch was not linear in relation to the potential application of this source of starch for 3D printing, with 1 h already sufficient to generate functionalized starches for this application. These characteristics are very important for future applications, mainly in the field of biomaterials.

With regard to reproducibility (Table 4), a smaller standard deviation is observed, in terms of weight and area, for the modified starches in relation to the native one. In addition, the GF_{area} and $GF_{orifices}$ of the printed material are greater for the DHT_1h and DHT_2h hydrogels, making the potential of these starches for this application even more evident. Therefore, the DHT time of 1 and 2 h improved the printability of the potato starch hydrogels, increasing the fidelity and reproducibility with the 3D design.

Previous works showed that, although starch is an interesting ingredient for 3D printing applications (bio-ink, biomaterials, food), some strategies are needed to allow good performance. One strategy is combining starch with other macromolecules, such as fruits [45], vegetables [46], proteins [12]/gelatin [47], or other polysaccharides, such as carrageenan [48]. However, those biopolymers are noble and/or expensive biomacromolecules, whose use only to improve the gelling properties of starch can be avoided. Therefore, starch modification can be an interesting strategy to achieve

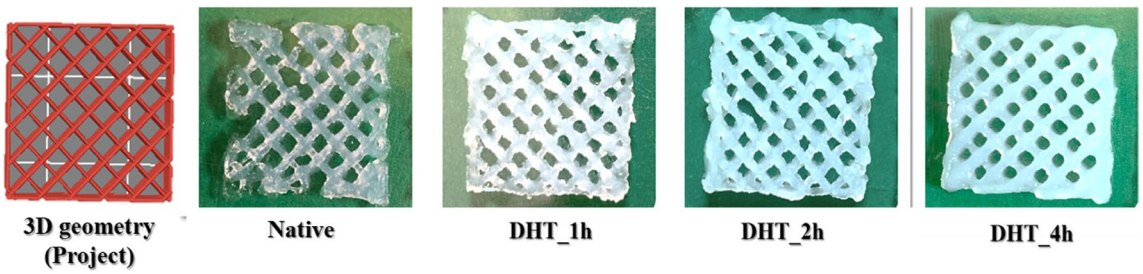

Fig. 4 Images of printed parallelepipeds based on native and modified potato starch hydrogels (DHT_1h, DHT_2h, and DHT_4h) to evaluate the 3D printing capability

Table 4 Reproducibility (weight, area, and number of orifices of the printed samples) and geometry fidelity (GF) in relation to area (GF_{area}) and number of orifices ($GF_{orifices}$) of the starch hydrogels printed in a parallelepiped shape. The hydrogels are based on control and modified starches by dry heating (DHT_1h, DHT_2h, and DHT_4h) (average ± standard deviation)

Samples	Weight (g)	Area-printed parallelepiped (cm^2)	Number of orifices	Geometry fidelity (GF) (%)	
				GF_{area}	$GF_{orifices}$
Native	0.5445 ± 0.0333^{C}	3.12 ± 0.54^{C}	24 ± 12^{C}	78 ± 12^{C}	77 ± 11^{B}
DHT_1h	0.5904 ± 0.0114^{A}	3.83 ± 0.21^{A}	44 ± 2^{A}	96 ± 4^{A}	90 ± 5^{A}
DHT_2h	0.5867 ± 0.0120^{A}	3.35 ± 0.36^{B}	42 ± 2^{A}	90 ± 4^{A}	93 ± 7^{A}
DHT_4h	0.5609 ± 0.0131^{B}	3.52 ± 0.24^{B}	31 ± 4^{B}	89 ± 6^{A}	90 ± 8^{A}

A, B, C: different letters indicate significant differences between native and the modified starches (DHT_1h, DHT_2h, and DHT_4h), as revealed by Tukey's test, $p < 0.05$. 3D-printed project parallelepiped shows 4 cm^2 of surface area and 88 orifices in its structure

better performance with commercial sources of starch for 3D printing applications.

For instance, starch modification treatments such as ozone, DHT, and pulsed electric field resulted in cassava starch's stronger hydrogels when compared with the native one, with better printability [16, 49, 50]. Still, cassava starch is a source known to produce fairly weak gels in comparison with other sources, and potato starch is the contrary [9].

In the present work, we observed that DHT can produce stronger or weaker potato starch hydrogels, depending on the processing conditions, and also show better printability. Therefore, we observed that hydrogels must exhibit adequate rheological performance to promote smooth extrusion through the nozzle and a stable printed layer to support subsequent ones without deformation or collapse. Processing potato starch by DHT at 1 and 2 h was the best condition to do so.

In general, the inks developed in this work were within the viscosity profile range that allows good printability, being neither too liquid nor too thick, making it difficult to extrude. In addition, when deposited on the surface, they showed the ability not to spread and maintain stability for the deposition of the next line.

As the next step, the produced bio-scaffolds were evaluated in terms of mechanical properties, biodegradability, and swelling power. These properties are fundamentals to evaluate the potential of these raw materials to be used for this biomedical application.

3.3 Bio-scaffold properties

Table 5 presents the mechanical properties of the snap-dried bio-scaffolds based on the starch hydrogels. The bio-scaffolds showed no significant difference in relation to the consistency (15 mm). However, bio-scaffolds based on modified starch hydrogels showed advanced resistance at break (60–80 MPa) and lower flexibility (35–65%) than that based on the native starch hydrogels—it is worth mentioning the applicability of this result. The time of dry heating treatment was not proportional to the mechanical properties, with DHT_1h resulting in the strongest and least flexible bio-scaffolds. As mentioned earlier, the process of dry heating leads to depolymerization and oxidation of starch molecules, resulting in the formation of carbonyl groups. Zhao et al. [51] explained that these carbonyl groups are available to form robust hydrogen bonds with the hydroxyl groups of starch, leading to the development of stiffer materials with reduced elongation. Additionally, depolymerization enhances the tendency of molecule re-association, potentially promoting stronger interactions [52]. Consequently, the newly formed polymeric matrix exhibits different molecular interactions among starch and water, ultimately resulting in the production of stronger scaffold materials.

Table 5 Mechanical properties and biodegradability of the bio-scaffolds based on native and modified potato starch hydrogels (DHT_1h, DHT_2h, and DHT_4h) (average ± standard deviation)

Samples	*F* (N)	*D* (mm)	Biodegradability (100%)	
			Estimated time in weeks	R^2
Native	50.35 ± 5.76^{c}	7.10 ± 1.06^{a}	5.61 ± 0.17^{d}	0.98
DHT_1h	90.63 ± 1.83^{a}	2.89 ± 0.55^{c}	9.19 ± 0.12^{a}	0.97
DHT_2h	83.20 ± 3.01^{b}	4.55 ± 0.88^{b}	6.03 ± 0.09^{c}	0.99
DHT_4h	80.00 ± 3.00^{b}	4.45 ± 0.62^{b}	6.88 ± 0.19^{b}	0.97

a, b, c, d: Different letters indicate significant differences between native and the modified starches (DHT_1h, DHT_2h, and DHT_4h), as revealed by Tukey's test, $p < 0.05$

F, puncture force (N); *D*, probe displacement (mm)

The starch bio-scaffolds produced in this work showed higher resistance at break (~ 10 x) and similar flexibility than molded collagen-carrageenan bio-scaffolds produced in the work of Nogueira et al. [53]. In addition, considering the area of the probe used for the mechanical tests (area = 7.1 × 10^{-6} mm^2, radius = 1.5 mm), the starch-based bio-scaffolds developed in this work supported stress of 7.09, 12.8, 11.7, and 11.3 MPa for native starch, DHT_1h, DHT_2h, and DHT_4h, respectively. Note that the values obtained are compatible with the tension supported by trabecular bone (2–12 MPa) indicating that these biomaterials have the potential to be used as bone bio-scaffolds [54].

In regenerative applications, it is essential for polymer-based bio-scaffolds to exhibit biodegradability, enabling the gradual replacement or remodeling of the scaffold with natural tissue, without leaving behind any solid materials in the body [55]. Figure 5 shows the degradation of bio-scaffolds as a function of the period that they were immersed in the cell culture medium (7 and 14 days). All the bio-scaffolds produced in this work showed biodegradability in the α-MEM medium; those made with modified starch showed slower biodegradability in the estimated period (with emphasis on DHT_1 h) than that grounded on native starch hydrogels. This aspect is interesting once following implantation, the scaffold must degrade in a timely manner to ensure proper remodeling of the tissue [56]. Bone tissue healing typically progresses through three distinct stages: the initial inflammatory phase, lasting approximately 3 to 7 days; the repair phase, spanning 3 to 4 months; and lastly, the ongoing remodeling phase, which can extend over several months to years [57]. Consequently, a competent bone implant should retain adequate mechanical strength for a minimum of 12 weeks. The biodegradation of the bone scaffold must be compatible with the cellular events underlying their integration with the host and the formation of new ones [58]. Inadequate degradation rates can significantly hinder the regenerative potential of biomaterials [59]. In

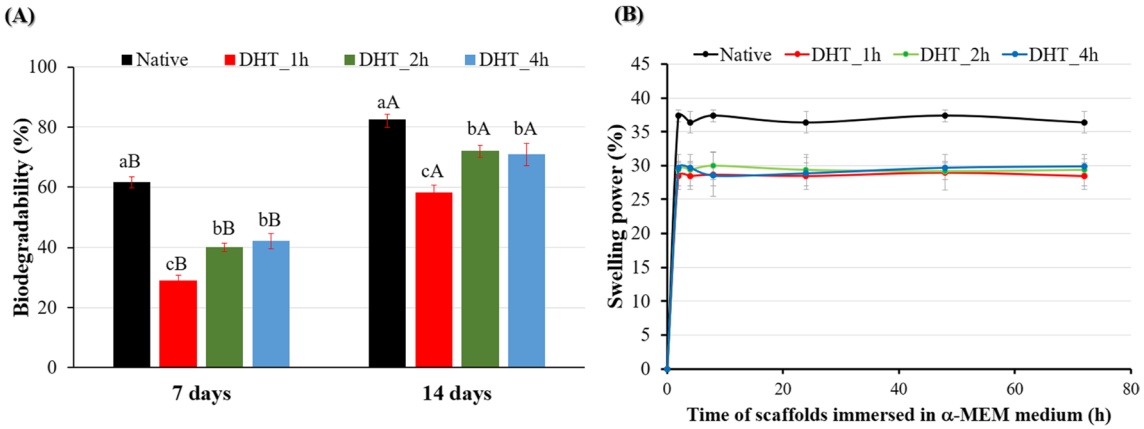

Fig. 5 Biodegradability (**A**) and swelling power (**B**) of the bio-scaffolds based on native and modified potato starch hydrogels (DHT_1h, DHT_2h, and DHT_4h) (average ± standard deviation). (A–C) Different letters indicate significant differences between native and the modified starches (DHT_1h, DHT_2h, and DHT_4h), as revealed by Tukey's test, $p < 0.05$

general, the 3D printed bio-scaffolds based on potato starch showed total biodegradability (100%) around to 5 until 9 weeks (Table 5 and Appendix 1), which is too fast considering this application. However, it is notable that the DHT promoted a significant reduction of the biodegradability rate bringing greater potential for use of this starch source in this application.

Also, as biodegradability impairs mechanical properties [57], the results indicate that modified starch-based bio-scaffolds can maintain their integrity for longer periods than native starch, which is interesting for bone regeneration.

In the literature, it was also observed that the biodegradability of materials made from modified starches, specifically acetylated and cross-linked variants, is lower compared to films made from their native counterparts [60]. This reduced biodegradability can be attributed to the increased interaction within the polymeric chains, resulting in a stronger network within the matrix. As a consequence, the number of available glucose OH groups that can bind to water molecules and facilitate biodegradation is reduced. However, it is important to highlight that the acetylated and cross-linked starches are produced by chemical reactions [60], contrary to the physical process of DHT proposed here.

All the starch bio-scaffolds produced in this work showed swelling when added to α-MEM medium, and these biomaterials reached their maximum swelling at the moment they were added to the medium—and it stabilized and remained relatively constant until 72 h (Fig. 5B). The bio-scaffolds based on native starch hydrogels exhibit slightly higher water absorption capacities compared to the modified starch hydrogels. This difference can be attributed to the hydrophilic sites present in the architecture of the bio-scaffolds, which contributes to their water retention capabilities. Swelling of bio-scaffolds in an aqueous medium can sometimes be desirable in biomedical applications because the pore size would initially increase and accommodate the cells, although scaffold swelling would lead to poorer mechanical properties [61]. The best behavior, thus, depends on the target application.

In general, the bio-scaffolds based on the modified starches showed superior properties than the native ones. These bio-scaffolds are mechanically stronger, are less biodegradable, and show lower swelling power, which is an important characteristic for this application, and these biomaterials must have integrity to be one adequate surface for cell adhesion and proliferation.

4 Conclusion

The "clean" technology and physical dry heating (DHT) proved to be effective in promoting changes in the potato starch structure, promoting slight oxidation (carbonyl formation) and partial depolymerization. These changes are reflected in changes in paste properties, rheology, and firmness of the hydrogel. Modified starches were able to form stronger (DHT_1h) or weaker (DHT_2h and DHT_4h) hydrogels when compared to the native source, depending on the process conditions. DHT-modified starches had improved printability (3D printed samples with more continuous lines, well-defined geometry of printed materials) when compared to native starch, with emphasis on 1 and 2 h that showed better resolution and reproducibility in terms of weight, area, and number of holes in the printed materials, increasing fidelity with the 3D design geometry. Furthermore, the starch modification suggested in this work resulted in printed bio-scaffolds with superior properties when compared to those based on native hydrogels. The bio-scaffolds based on modified starches showed superior mechanical properties, lower rate of biodegradability, and

swelling power. We can conclude that DHT_1h was the best option to be used as a gelling ingredient to produce 3D-printed bio-scaffolds. Therefore, it can be said that the potato starch modified by DHT overcame the deficiencies found in the native potato starch, becoming a promising ingredient to be used as "inks" for printing functional biomaterials. The information obtained in this work can also be useful to expand future applications for potato starch, focusing mainly on potential biomaterials such as bone bioscaffolds produced via additive manufacturing. Finally, this work opens new possibilities for using natural biopolymers for biomedical applications, the reason why we consider it relevant from both academic and industrial points of view.

Appendix 1

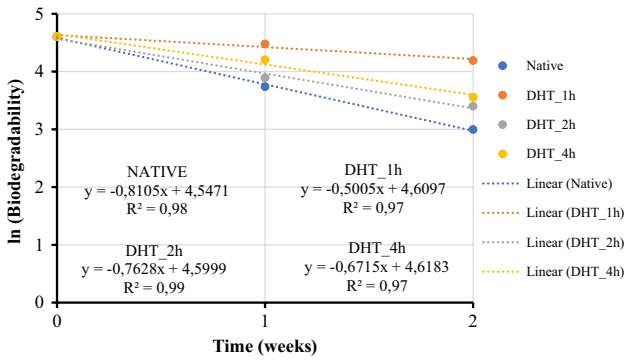

Evolution of the biodegradability during the evaluated period (7 and 14 days, 1 and 2 weeks, respectively).

Acknowledgments The authors are grateful to the "Fundação de Amparo a Pesquisa do Estado de São Paulo – FAPESP" for funding the projects n° 2019/25054-2 and 2020/08727-0 and for financing the BC Maniglia Young Investigator grant (2021/05947-2) and the JS Guedes Ph.D. scholarship (2021/06398-2), the National Council for Scientific and Technological Development (CNPq, Brazil) for funding the PAI Sponchiado Master scholarship (162334/2021-4), the PRP/USP for funding the project PIPAE 2021.1.1024.1.9, the "Coordenação de Aperfeiçoamento de Pessoal de Nível Superior – Brasil (CAPES)"—for financing the BS Bitencourt PhD scholarship (88887.636998/2021-00), and the CAPES/Brazil and COFECUB/France for funding the project Ph 1006/23 (CAPES code 001). Communauté urbaine du Grand Reims, Département de la Marne, Région Grand Est, and European Union (FEDER Champagne-Ardenne 2014-2020) are acknowledged for their financial support to the Chair of Biotechnology of CentraleSupélec and the Centre Européen de Biotechnologie et de Bioéconomie (CEBB).

Authors' contributions Pedro Augusto Invernizzi Sponchiado: conceptualization, methodology, validation, formal analysis, investigation, data curation, writing—original draft, and visualization. **Maryanne Trafani de Melo**: methodology, validation, formal analysis, investigation, visualization, data curation, writing—review, and editing. Bruna Sousa Bitencourt: methodology, validation, investigation, and data curation. **Jaqueline Souza Guedes**: methodology, validation, investigation, and data curation. **Delia Rita Tapia-Blácido:** resources, methodology, writing—review, and editing. **Pedro Esteves Duarte Augusto**: resources, methodology, formal analysis, writing—review, editing, and supervision. **Ana Paula Ramos**: resources, methodology, formal analysis, writing—review, editing, supervision, project administration, and funding acquisition**. Bianca Chieregato Maniglia:** conceptualization, methodology, validation, formal analysis, resources, writing—original draft, writing—review, editing, supervision, project administration, and funding acquisition.

Declarations

Conflict of interests The authors declare no competing interests.

References

1. J.C. Boga, S.P. Miguel, D. de Melo-Diogo, A.G. Mendonça, R.O. Louro, I.J. Correia, In vitro characterization of 3D printed scaffolds aimed at bone tissue regeneration. Colloids. Surf. B. Biointerfaces. **165**, 207–218 (2018). https://doi.org/10.1016/j.colsurfb.2018.02.038
2. S. Naghieh, M. Sarker, N.K. Sharma, Z. Barhoumi, X. Chen, Printability of 3D printed hydrogel scaffolds: Influence of hydrogel composition and printing parameters. Appl. Sci. **10**, 292 (2019). https://doi.org/10.3390/app10010292
3. M. Askari, M. Afzali Naniz, M. Kouhi, A. Saberi, A. Zolfagharian, M. Bodaghi, Recent progress in extrusion 3D bioprinting of hydrogel biomaterials for tissue regeneration: A comprehensive review with focus on advanced fabrication techniques. Biomater. Sci. **9**, 535–573 (2021). https://doi.org/10.1039/D0BM00973C
4. A. Dhawan, P.M. Kennedy, E.B. Rizk, I.T. Ozbolat, Three-dimensional bioprinting for bone and cartilage restoration in orthopaedic surgery. J. Am. Acad. Orthopaed. Surg. **27**, e215–e226 (2019). https://doi.org/10.5435/JAAOS-D-17-00632
5. A. Iglesias-Mejuto, C.A. García-González, 3D-printed alginate-hydroxyapatite aerogel scaffolds for bone tissue engineering. Mater. Sci. Eng : C **131**, 112525 (2021). https://doi.org/10.1016/j.msec.2021.112525
6. M.R. Roslan, N.F.M. Nasir, E.M. Cheng, N.A.M. Amin, Tissue engineering scaffold based on starch: A review, in: International Conference on Electrical, Electronics, and Optimization Techniques (ICEEOT). IEEE., 1857–1860 (2016). https://doi.org/10.1109/ICEEOT.2016.7755010
7. X. Shi, J. Gao, Q. Lv, H. Cai, F. Wang, R. Ye, X. Liu, Calcification in atherosclerotic plaque vulnerability: friend or foe? Front. Physiol. **11**, 1–12 (2020). https://doi.org/10.3389/fphys.2020.00056
8. B. Mahendiran, S. Muthusamy, S. Sampath, S.N. Jaisankar, K.C. Popat, R. Selvakumar, G.S. Krishnakumar, Recent trends in natural polysaccharide based bioinks for multiscale 3D printing in tissue regeneration: A review. Int. J. Biol. Macromol. **183**, 564–588 (2021). https://doi.org/10.1016/j.ijbiomac.2021.04.179
9. B.C. Maniglia, N. Castanha, P. Le-Bail, A. Le-Bail, P.E.D. Augusto, Starch modification through environmentally friendly alternatives: A review. Crit. Rev. Food. Sci. Nutr., 1–24 (2020). https://doi.org/10.1080/10408398.2020.1778633
10. X. Zeng, H. Chen, L. Chen, B. Zheng, Insights into the relationship between structure and rheological properties of starch gels in hot-extrusion 3D printing. Food. Chem. **342**, 128362 (2021). https://doi.org/10.1016/j.foodchem.2020.128362
11. S. Ma, J. Liu, Q. Zhang, Q. Lin, R. Liu, Y. Xing, H. Jiang, 3D printing performance using radio frequency electromagnetic wave

modified potato starch. Inn. Food. Sci. Emerg. Technol., 103064 (2022). https://doi.org/10.1016/j.ifset.2022.103064
12. F. Chuanxing, W. Qi, L. Hui, Z. Quancheng, M. Wang, Effects of pea protein on the properties of potato starch-based 3D printing materials. Int. J. Food. Eng. **14** (2018). https://doi.org/10.1515/ijfe-2017-0297
13. B. Chieregato Maniglia, T. Carregari Polachini, E.-A. Norwood, P. Le-Bail, A. Le-Bail, Thermal technologies to enhance starch performance and starchy products. Curr. Opin. Food. Sci. **40**, 72–80 (2021). https://doi.org/10.1016/j.cofs.2021.01.005
14. N. Lei, S. Chai, M. Xu, J. Ji, H. Mao, S. Yan, Y. Gao, H. Li, J. Wang, B. Sun, Effect of dry heating treatment on multi-levels of structure and physicochemical properties of maize starch: A thermodynamic study. Int. J. Biol. Macromol. **147**, 109–116 (2020). https://doi.org/10.1016/j.ijbiomac.2020.01.060
15. S. Liang, C. Su, A.S.M. Saleh, H. Wu, B. Zhang, X. Ge, W. Li, Repeated and continuous dry heat treatments induce changes in physicochemical and digestive properties of mung bean starch. J. Food. Process. Preserv. **45**, e15281 (2021)
16. B.C. Maniglia, D.C. Lima, M.D. Matta Junior, P. Le-Bail, A. Le-Bail, P.E.D. Augusto, Preparation of cassava starch hydrogels for application in 3D printing using dry heating treatment (DHT): A prospective study on the effects of DHT and gelatinization conditions. Food. Res. Int. **128**, 108803 (2020). https://doi.org/10.1016/j.foodres.2019.108803
17. B.C. Maniglia, D.C. Lima, M. da Matta Júnior, A. Oge, P. Le-Bail, P.E.D. Augusto, A. Le-Bail, Dry heating treatment: A potential tool to improve the wheat starch properties for 3D food printing application. Food. Res. Int. **137**, 109731 (2020). https://doi.org/10.1016/j.foodres.2020.109731
18. I.K. Oh, I.Y. Bae, H.G. Lee, Effect of dry heat treatment on physical property and in vitro starch digestibility of high amylose rice starch. Int. J. Biol. Macromol. **108**, 568–575 (2018). https://doi.org/10.1016/j.ijbiomac.2017.11.180
19. T. Vasanthan, W. Bergthaller, D. Driedger, J. Yeung, P. Sporns, Starch from Alberta potatoes: Wet-isolation and some physicochemical properties. Food. Res. Int. **32**, 355–365 (1999). https://doi.org/10.1016/S0963-9969(99)00096-4
20. Y. Song, J. Jane, Characterization of barley starches of waxy, normal, and high amylose varieties. Carbohydr. Polym. **41**, 365–377 (2000). https://doi.org/10.1016/S0144-8617(99)00098-3
21. B.O. Juliano, A simplified assay for milled-rice amylose. Cereal. Sci. Today. **16**, 334–340 (1971)
22. R.J. Smith, Production and use of hypochlorite oxidized starches. Starch. Chem. Technol. **2**, 620–625 (1967)
23. S. Chattopadhyay, R.S. Singhal, P.R. Kulkarni, Optimisation of conditions of synthesis of oxidised starch from corn and amaranth for use in film-forming applications. Carbohydr. Polym. **34**, 203–212 (1997). https://doi.org/10.1016/S0144-8617(97)87306-7
24. D.C. Lima, B.C. Maniglia, M.D. Matta Junior, P. Le-Bail, A. Le-Bail, P.E.D. Augusto, Dual-process of starch modification: Combining ozone and dry heating treatments to modify cassava starch structure and functionality. Int. J. Biol. Macromol. **167**, 894–905 (2021). https://doi.org/10.1016/j.ijbiomac.2020.11.046
25. P.D. Sobral, F.C. Menegalli, M.D. Hubinger, M.A. Roques, Mechanical, water vapor barrier and thermal properties of gelatin based edible films. Food. Hydrocoll. **15**, 423–432 (2001)
26. C.I.A. La Fuente, A.T. de Souza, C.C. Tadini, P.E.D. Augusto, Ozonation of cassava starch to produce biodegradable films. Int. J. Biol. Macromol. **141**, 713–720 (2019). https://doi.org/10.1016/j.ijbiomac.2019.09.028
27. P.E.D.. GUEDES, J. S. ; BITENCOURT, B. S. ; Augusto, Modified maize starch for 3D printing of food analogues for people with dysphagia: Evaluation of texture profile and IDDSI method., in: 5th ISEKI E-Conference: Current Food Innovation Trends; the Texture and Consumer Perception Perspective, 2022., 2022.
28. S. Balet, A. Guelpa, G. Fox, M. Manley, Rapid Visco Analyser (RVA) as a tool for measuring starch-related physiochemical properties in cereals: A review, Food Anal Methods 12 (2019) 2344–2360.
29. N. Castanha, M.D. da Matta Junior, P.E.D. Augusto, Potato starch modification using the ozone technology. Food. Hydrocoll. **66**, 343–356 (2017). https://doi.org/10.1016/j.foodhyd.2016.12.001
30. D. Cozzolino, The use of the rapid visco analyser (RVA) in breeding and selection of cereals. J. Cereal. Sci. **70**, 282–290 (2016). https://doi.org/10.1016/j.jcs.2016.07.003
31. Z. Liu, H. Chen, B. Zheng, F. Xie, L. Chen, Understanding the structure and rheological properties of potato starch induced by hot-extrusion 3D printing. Food. Hydrocoll. **105812** (2020)
32. R. Mu, B. Wang, W. Lv, J. Yu, G. Li, Improvement of extrudability and self-support of emulsion-filled starch gel for 3D printing: Increasing oil content. Carbohyd. Polym. **301**, 120293 (2023). https://doi.org/10.1016/j.carbpol.2022.120293
33. A. Le-Bail, B.C. Maniglia, P. Le-Bail, Recent advances and future perspective in additive manufacturing of foods based on 3D printing. Curr. Opin. Food. Sci. **35**, 54–64 (2020). https://doi.org/10.1016/j.cofs.2020.01.009
34. M. Bercea, Rheology as a tool for fine-tuning the properties of printable bioinspired gels. Molecules. **28**, 2766 (2023). https://doi.org/10.3390/molecules28062766
35. Y. Cheng, Y. Fu, L. Ma, P.L. Yap, D. Losic, H. Wang, Y. Zhang, Rheology of edible food inks from 2D/3D/4D printing, and its role in future 5D/6D printing. Food. Hydrocoll. **132**, 107855 (2022). https://doi.org/10.1016/j.foodhyd.2022.107855
36. Q. Liu, N. Zhang, W. Wei, X. Hu, Y. Tan, Y. Yu, Y. Deng, C. Bi, L. Zhang, H. Zhang, Assessing the dynamic extrusion-based 3D printing process for power-law fluid using numerical simulation. J. Food Eng. **275**, 109861 (2020). https://doi.org/10.1016/j.jfoodeng.2019.109861
37. S.V. Murphy, A. Atala, 3D bioprinting of tissues and organs. Nat. Biotechnol. **32**, 773–785 (2014). https://doi.org/10.1038/nbt.2958
38. S. Ahn, J. Byun, H. Joo, J. Jeong, D. Lee, K. Cho, 4D printing of continuous shape representation. Adv. Mater. Technol. **6**, 2100133 (2021). https://doi.org/10.1002/admt.202100133
39. X. Li, L. Fan, Y. Liu, J. Li, New insights into food O/W emulsion gels: Strategies of reinforcing mechanical properties and outlook of being applied to food 3D printing. Crit. Rev. Food. Sci. Nutr. **63**, 1564–1586 (2023). https://doi.org/10.1080/10408398.2021.1965953
40. M. Deptuła, M. Zawrzykraj, J. Sawicka, A. Banach-Kopeć, R. Tylingo, M. Pikuła, Application of 3D- printed hydrogels in wound healing and regenerative medicine. Biomed. Pharmacother. **167**, 115416 (2023). https://doi.org/10.1016/j.biopha.2023.115416
41. H. Chen, F. Xie, L. Chen, B. Zheng, Effect of rheological properties of potato, rice and corn starches on their hot-extrusion 3D printing behaviors. J. Food. Eng. **244**, 150–158 (2019). https://doi.org/10.1016/j.jfoodeng.2018.09.011
42. Y. Cheng, H. Qin, N.C. Acevedo, X. Jiang, X. Shi, 3D printing of extended-release tablets of theophylline using hydroxypropyl methylcellulose (HPMC) hydrogels. Int. J. Pharmaceut. **591**, 119983 (2020). https://doi.org/10.1016/j.ijpharm.2020.119983
43. D. Petta, U. D'Amora, L. Ambrosio, D.W. Grijpma, D. Eglin, M. D'Este, Hyaluronic acid as a bioink for extrusion-based 3D printing. Biofab. **12**, 032001 (2020). https://doi.org/10.1088/1758-5090/ab8752
44. A. Pössl, D. Hartzke, T.M. Schmidts, F.E. Runkel, P. Schlupp, A targeted rheological bioink development guideline and its systematic correlation with printing behavior. Biofab. **13**, 035021 (2021). https://doi.org/10.1088/1758-5090/abde1e

45. I. Tomašević, P. Putnik, F. Valjak, B. Pavlić, B. Šojić, A. Bebek Markovinović, D. Bursać Kovačević, 3D printing as novel tool for fruit-based functional food production. Curr. Opin. Food. Sci. **41**, 138–145 (2021). https://doi.org/10.1016/j.cofs.2021.03.015
46. C. Guo, M. Zhang, B. Bhandari, S. Devahastin, Investigation on simultaneous change of deformation, color and aroma of 4D printed starch-based pastes from fruit and vegetable as induced by microwave. Food. Res. Int. **157**, 111214 (2022). https://doi.org/10.1016/j.foodres.2022.111214
47. A.G. Sartori, A.S. Saliba, B.S. Bitencourt, J.S. Guedes, L.C. Torres, S.M. Alencar, P.E. Augusto, Anthocyanin bioaccessibility and anti-inflammatory activity of a grape-based 3D printed food for dysphagia. Inn. Food Sci. Emerg. Technol. **84**, 103289 (2023). https://doi.org/10.1016/j.ifset.2023.103289
48. B.S. Bitencourt, J.S. Guedes, A.S.M.C. Saliba, A.G.O. Sartori, L.C.R. Torres, J.E.P.G. Amaral, S.M. Alencar, B.C. Maniglia, P.E.D. Augusto, Mineral bioaccessibility in 3D printed gels based on milk/starch/κ-carrageenan for dysphagic people. Food. Res. Int. **170**, 113010 (2023). https://doi.org/10.1016/j.foodres.2023.113010
49. B.C. Maniglia, D.C. Lima, M.D. Matta Junior, P. Le-Bail, A. Le-Bail, P.E.D. Augusto, Hydrogels based on ozonated cassava starch: Effect of ozone processing and gelatinization conditions on enhancing 3D-printing applications. Int. J. Biol. Macromol. **138**, 1087–1097 (2019). https://doi.org/10.1016/j.ijbiomac.2019.07.124
50. B.C. Maniglia, G. Pataro, G. Ferrari, P.E.D. Augusto, P. Le-Bail, A. Le-Bail, Pulsed electric fields (PEF) treatment to enhance starch 3D printing application: Effect on structure, properties, and functionality of wheat and cassava starches. Inn. Food. Sci. Emerg. Technol. **68**, 102602 (2021). https://doi.org/10.1016/j.ifset.2021.102602
51. Z. Zhao, Q. Wang, B. Yan, W. Gao, X. Jiao, J. Huang, J. Zhao, H. Zhang, W. Chen, D. Fan, Synergistic effect of microwave 3D print and transglutaminase on the self-gelation of surimi during printing. Inn. Food. Sci. Emerg. Technol. **67**, 102546 (2021). https://doi.org/10.1016/j.ifset.2020.102546
52. J.S. Guedes, K.C. Santos, N. Castanha, M.L. Rojas, M.D. Matta Junior, D.C. Lima, P.E.D. Augusto, Structural modification on potato tissue and starch using ethanol pre-treatment and drying process. Food. Struct. **29**, 100202 (2021). https://doi.org/10.1016/j.foostr.2021.100202
53. L.F.B. Nogueira, M.A.E. Cruz, M.T. de Melo, B.C. Maniglia, F. Caroleo, R. Paolesse, H.B. Lopes, M.M. Beloti, P. Ciancaglini, A.P. Ramos, M. Bottini, Collagen/κ-carrageenan-based scaffolds as biomimetic constructs for in vitro bone mineralization studies. Biomacromol. **24**, 1258–1266 (2023). https://doi.org/10.1021/acs.biomac.2c01313
54. Q. Fu, E. Saiz, M.N. Rahaman, A.P. Tomsia, Toward strong and tough glass and ceramic scaffolds for bone repair. Adv. Funct. Mater. **23**, 5461–5476 (2013). https://doi.org/10.1002/adfm.201301121
55. H.-J. Sung, C. Meredith, C. Johnson, Z.S. Galis, The effect of scaffold degradation rate on three-dimensional cell growth and angiogenesis. Biomater. **25**, 5735–5742 (2004). https://doi.org/10.1016/j.biomaterials.2004.01.066
56. A.V. Vasiliadis, K. Katakalos, The role of scaffolds in tendon tissue engineering. J. Funct. Biomater. **11**, 78 (2020). https://doi.org/10.3390/jfb11040078
57. S. Wei, J.-X. Ma, L. Xu, X.-S. Gu, X.-L. Ma, Biodegradable materials for bone defect repair. Mil. Med. Res. **7**, 54 (2020). https://doi.org/10.1186/s40779-020-00280-6
58. F. Bornert, V. Herber, R. Sandgren, L. Witek, P.G. Coelho, B.E. Pippenger, S. Shahdad, Comparative barrier membrane degradation over time: Pericardium versus dermal membranes. Clin. Exp. Dent. Res. **7**, 711–718 (2021). https://doi.org/10.1002/cre2.414
59. M. Qasim, D.S. Chae, N. Lee, Advancements and frontiers in nano-based 3D and 4D scaffolds for bone and cartilage tissue engineering. Int. J. Nanomed. **14**, 4333–4351 (2019). https://doi.org/10.2147/IJN.S209431
60. R.A. González-Soto, M.C. Núñez-Santiago, L.A. Bello-Pérez, Preparation and partial characterization of films made with dual-modified (acetylation and crosslinking) potato starch. J. Sci. Food. Agric. **99**, 3134–3141 (2019). https://doi.org/10.1002/jsfa.9528
61. R.M. Felfel, M.J. Gideon-Adeniyi, K.M.Z. Hossain, G.A.F. Roberts, D.M. Grant, Structural, mechanical and swelling characteristics of 3D scaffolds from chitosan-agarose blends. Carbohydr. Polym. **204**, 59–67 (2019)